MATEMATIKA, MJIAM, Volume 41, Number 3, 375–387


# Bifurcation Analysis of a Modified SIR-Based COVID-19 Model with Nonlinear Incidence and Recovery Rates

[1,2]Abubakar Shehu Sidi and [1]Mohd Hafiz Mohd*

[1]School of Mathematical Sciences, Universiti Sains Malaysia, 11800 USM, Penang, Malaysia.
[2]Umaru Ali Shinkafi Polytechnic, Sokoto, Nigeria.
*Corresponding author: mohdhafizmohd@usm.edu.my

Article history
Received: 7 February 2025
Received in revised form: 5 June 2025
Accepted: 4 August 2025
Published on line: 15 November 2025

**Abstract** In this work, a Susceptible-Infected-Recovered ($SIR$)-based epidemic model incorporating nonlinear incidence and recovery rates, with the consideration of limited medical resources (e.g., the availability of hospital beds) is examined. The model also emphasises the significance of factoring in distinct intervention strategies and considers some important epidemiological factors, in the light of COVID-19 endemicity. In particular, the study employs a Monod-type nonlinear incidence rate coupled with a nonlinear recovery equation, to uncover the intricate dynamics that emerge from the interplay of these epidemiological forces. The findings reveal the existence of disease-free and endemic equilibria, their stability conditions, and bifurcational changes in the dynamics of the system. Bifurcation analysis demonstrates the emergence of transcritical, saddle-node and Hopf bifurcations with the existence of distinct stable and unstable equilibria and limit cycles. Overall, this work highlights the importance of mathematical modeling and dynamical systems techniques in investigating the interplay among various epidemiological factors, thereby providing valuable insights to guide effective epidemic control strategies.

**Keywords** COVID-19, nonlinear incidence and recovery rates, dynamical systems, bifurcation analysis, equilibria.

**Mathematics Subject Classification** 37G35, 34C23.

## 1 Introduction

Over the years infectious diseases ranging from olden days plagues and European black deaths down to the present pandemics have been a serious health threat to both humans and nonhuman globally [5], causing many casualties and numerous deaths. Mathematical models contribute immensely to examining the dynamics of infectious diseases such as malaria, Ebola, dengue fever, SARS-COV2 [7] and providing health policymakers with information to help design strategies for containing epidemics. According to [6], different mathematical models considered important epidemiological factors like demography, population size, mixing patterns, diseases' latency period, transmission and recovery rates, etc. The analysis of these models reveals vital

insights into the spread patterns of infectious diseases and estimation of basic reproduction number, $R_0$.

Apart from the quantity $R_0$, the epidemiological functions that define the incidence and recovery rates are among the primary factors that determine a model's behavior in infectious disease modelling. To expand on research and improve comprehension of the saturation effect and limited healthcare resources, distinct studies such as [1, 3, 8, 9, 15] incorporated nonlinear incidence and recovery rates into the $SIR$ model. This prevented the recovery rate from declining as the number of infectious individuals increased and controlled the rise in new cases. Considering nonlinear incidence and recovery rates in the $SIR$ model is a means of uncovering some vital dynamics. The nonlinear incidence rate often being given by:

$$\frac{\beta SI}{1+\alpha I},$$

where $\beta$ is the transmission rate, $S$ is the number of susceptible individuals, $I$ is the number of infectious individuals, and $\alpha$ is a parameter that regulates the saturation effect [1]. The recovery rate can be modelled as follows:

$$\frac{\gamma I}{1+\delta I},$$

where $\gamma$ is the recovery rate and $\delta$ is a parameter controlling the effect of healthcare saturation [4]. Previous investigations, such as [11], employed an ordinary differential equations (ODE) model incorporating the nonlinear epidemiological functions to demonstrate the existence of forward and backward bifurcations in the analysis of the COVID-19 $SEIR$ system. Their findings on the bifurcation analysis further reveal that by implementing drastic preventive measures during epidemic outbreaks, consequently, this situation can reduce $R_0$, which can help policymakers effectively control the spread of disease [11]. The co-infection of HIV and COVID-19 model developed by [12] also exhibits backward bifurcation when $R_0$ is below than unity; this finding implies that backward bifurcation can result in multiple equilibria, which may explain the persistence of a stable endemic state. Additionally, [14] contributed to the understanding of a modified $SIR$ model where the susceptible population undergoes logistic growth while being vaccinated at a constant rate; their analysis shows that the model's endemic equilibrium displays distinct codimension 1 and codimension 2 bifurcations. This study also highlights the importance of vaccination parameter by deriving an expression for the number of individuals that need to be vaccinated to reduce disease transmission [14].

Another modelling work by [10] employed the SEIQHR fractional epidemic model to deepen investigation and enhance the understanding of the epidemiological insights into the spreading dynamics of infectious disease. Their analysis illustrated the impact of the model parameters and memory effects on the transmission dynamics by presenting conditions for the occurrence of both forward and backward bifurcations [10]. Unlike the classical ODE (or integer-order) models, fractional-order models effectively incorporate memory and historical effects across different stages of an epidemic, thereby offering an alternative framework framework for identifying stability conditions and bifurcation scenarios in complex disease transmission dynamics [17, 18]. Additionally, the application of dynamical systems techniques and bifurcation theory, along with the consideration of discrete-time modelling framework, enabled [9] to prove the existence of different codimension 1 and codimension 2 bifurcations; this study concludes that discrete-time models predict more complex dynamics compared to continuous-time epidemic models.

In a related study, [1] extends the classical SIR model by incorporating a Monod-equation type of nonlinear incidence rate, providing insights into the effects of intervention levels on infectious disease transmission. This incidence rate function suggests that, at low levels of infection, the rate remains low due to stringent interventions but escalates as the number of infected individuals increases, eventually reaching a state where it becomes independent of the infected subpopulation, as seen during the COVID-19 pandemic. Motivated by the work of [1], we employ numerical bifurcation analysis to examine the overall dynamics of the epidemiological system and we extend previous observations by broadening the numerical investigations regarding the parameter regime where disease persists or dies out.

This paper is organised as follows. Section 2 describes the $SIR$ model inspired by the work of [1]. Section 3 outlines the existence and stability analysis of the equilibria. Section 4 discusses codimension 1 bifurcation analysis results while also focuses on codimension 2 bifurcation analysis findings and the overall dynamics of the model. Finally, Section 5 concludes this study by highlighting the salient observations and further insights from the findings of this epidemiological system.

## 2 Model Description

The epidemiological system that has been considered in this study is inspired by [1]. The total population, $N(t)$, is divided into three subpopulations namely; Susceptible class, $S(t)$, Infected class, $I(t)$, and Recovered class, $R(t)$. Firstly, births occur at a constant rate $A$. Then, susceptible individuals get infected at the rate $\beta/(k+I)$, where $\beta$ is the transmission rate, $\beta IS$ is the force of infection and $k$ stands for the level of intervention. Additionally, infected individuals recover at the rate $(\alpha_0-(\alpha_1-\alpha_0)\frac{b}{(b+I)})$, where $b$ is the hospital bed population ratio, $\alpha_0$ and $\alpha_1$ are the respective minimum and maximum recovery rates. Finally, deaths can occur at the rate $(\gamma+\mu)$ where, $\mu$ denotes the natural death rate and $\gamma$ represents the disease-induced death rate. The schematic diagram in Figure 1 below described the transmission kinetics of the epidemiological system:

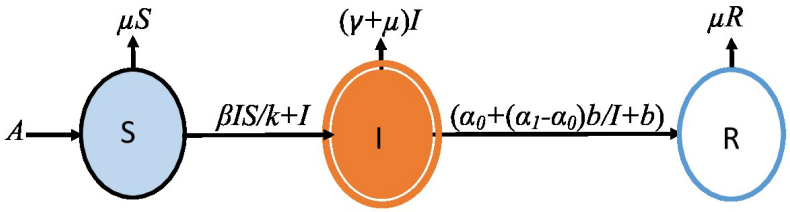


Figure 1: Schematic diagram of the epidemiological system with nonlinear incidence and recovery rates.

In general, this model extends the classical SIR framework by introducing nonlinear incidence and recovery rates. This nonlinear formulation enables the system to capture realistic epidemiological features such as saturation effects, healthcare capacity limits and intervention-induced behavioral modifications that are not adequately represented in the standard bilinear incidence $\beta SI$ or constant recovery rate models in the classical SIR.

Additionally, the nonlinear incidence term $\beta IS/(k+I)$, generalises the classical $\beta SI$ form by introducing a saturation denominator $(k+I)$. The parameter $k$ represents the intervention or control measure level, which can include vaccination, social distancing, or treatment capacity. As the number of infected individuals increases, the effective transmission rate saturates, reflecting the reduced contact efficiency due to awareness or behavioral adaptation within the population.

Another salient feature of the epidemiological system lies in the nonlinear recovery rate where $b$ denotes the hospital bed ratio and $\alpha_0$, $\alpha_1$ are the minimum and maximum recovery rates, respectively. This component models the healthcare system's saturation: at very low infected levels, $I$, the recovery rate approximates $\alpha_1$ (efficient recovery due to sufficient hospital capacity), whereas at very high infected levels, the recovery rate approaches $\alpha_0$ (poor recovery due to hospital overload). Hence, the model captures the real-world constraint that recovery efficiency declines when the number of infected individuals surpasses medical capacity.

## 3 Model Equations

Below is a system of nonlinear ordinary differential equations describing the model presented in Figure 1 above.

$$\frac{dS}{dt} = A - \frac{\beta SI}{k+I} - \mu S, \tag{1}$$

$$\frac{dI}{dt} = \frac{\beta SI}{k+I} - \left(\alpha_0 + (\alpha_1 - \alpha_0)\frac{b}{b+I}\right) I - (\gamma+\mu)I, \tag{2}$$

$$\frac{dR}{dt} = \left(\alpha_0 + (\alpha_1 - \alpha_0)\frac{b}{b+I}\right) I - \mu R. \tag{3}$$

The per capita recovery rate, $\alpha(b, I)$, is defined as:

$$\alpha(b, I) = \alpha_0 + (\alpha_1 - \alpha_0)\frac{b}{b+I}, \tag{4}$$

where $\alpha_0$ and $\alpha_1$ represent the minimum and maximum recovery rates, respectively. The formulation of equation (4) is inspired by the previous study of [2] and interested readers are referred to this work on the salient features of the recovery rate function. Since $R$ did not appear in equations (1)-(2), it is sufficient to use system (5)-(6) for this analysis:

$$\frac{dS}{dt} = A - \frac{\beta SI}{k+I} - \mu S, \tag{5}$$

$$\frac{dI}{dt} = \frac{\beta SI}{k+I} - \left(\alpha_0 + (\alpha_1 - \alpha_0)\frac{b}{b+I}\right) I - (\gamma+\mu)I. \tag{6}$$

Based on equations (5)-(6), the solution of the epidemiological system can be shown to be bounded, as follows:

$$\frac{dN}{dt} = A - \mu N(t) - \alpha(b, I)I - \gamma I(t), \tag{7}$$

$$N(t) \leq N(0)e^{-\mu t} + \frac{A}{\mu}(1 - e^{-\mu t}), \tag{8}$$

$$\lim_{t\to\infty} N(t) \leq \frac{A}{\mu}, \quad \text{and} \quad \dot{N} < 0, \quad \text{if} \quad N > \frac{A}{\mu}. \tag{9}$$

Thus, $N(t)$ is bounded and every solution of the system lies within a finite region. It can also be demonstrated that the solutions of this epidemiological system lie in the positively invariant region i.e., we define the feasible region as:

$$\Omega = \{(S(t), I(t)) \in \mathbb{R}^2_+ \cup \{0\} : S(t) + I(t) \leq \frac{A}{\mu}, t \geq 0\}. \tag{10}$$

From Equation (9), the total population cannot exceed $A/\mu$, since $\dot{N} < 0$ whenever $N > A/\mu$. Therefore, $\Omega$ is positively invariant, i.e., any positive trajectory starting in $\Omega$ remains in $\Omega$ for all $t \geq 0$:

$$(S(0), I(0)) \in \Omega \quad \Rightarrow \quad (S(t), I(t)) \in \Omega \quad \forall t \geq 0.$$

Furthermore, $\Omega$ is an absorbing set i.e., any trajectory with arbitrary nonnegative initial conditions eventually enters $\Omega$ and remains there permanently.

Biologically, the boundedness of $N(t)$ ensures that the total population never grows unboundedly, while the positive invariance of $\Omega$ guarantees epidemiological feasibility of all trajectories. Biologically, this means that the disease and population dynamics remain within realistic limits governed by demographic balance ($A/\mu$) and natural plus disease-induced mortality. This property is essential for subsequent analysis of equilibria, basic reproduction number and bifurcation analysis.

## 4 Existence of Equilibria and Stability Analysis

### 4.1 Disease-Free ($E_0$) and Endemic Equilibra ($E_1$)

To establish the presence of equilibrium points within the model defined by system (5)-(6), we equate the time derivatives of Susceptible ($S$) and Infected ($I$) populations to zero. This process yields the following set of equations:

$$A - \frac{\beta SI}{k + I} - \mu S = 0, \tag{11}$$

$$\frac{\beta SI}{k + I} - \left(\alpha_0 + (\alpha_1 - \alpha_0)\frac{b}{b + I}\right) I - (\gamma + \mu)I = 0. \tag{12}$$

A disease-free equilibrium (DFE) emerges when $I = 0$, yielding $S = \frac{A}{\mu}$ and this is denoted as $E_0 = \left(\frac{A}{\mu}, 0\right)$. At this equilibrium, the system exhibits maximal recovery alongside optimal susceptibility to the infection. An endemic equilibrium (EE) can also be calculated by solving the nonlinear simultaneous equations, which yields $E_1 = (S^*, I^*)$. We refer interested readers to the work of [1] on the stability analysis results of these equilibria.

To further examine the model's dynamics, this study established the derivation of the basic reproduction number, $R_0$, a pivotal metric in epidemiological models. This quantity highlights the (on-average) number of secondary cases produced by a primary index case in a wholly susceptible population. Employing the next-generation matrix method at $E_0$, where $\alpha(b, I)$ approaches $\alpha_1$ asymptotically, we compute $R_0$ by taking $F = \left(\frac{\beta A}{k\mu}\right)$ and $V = (\alpha_1 + \gamma + \mu)$. Then, the basic reproduction number $R_0$ is derived as the spectral radius of $FV^{-1}$, which simplifies to:

$$R_0 = \frac{\beta A}{k\mu(\alpha_1 + \gamma + \mu)}. \tag{13}$$

The formulation of $R_0$ highlights its reliance on the parameters governing the transmission rate ($\beta$), the intervention intensity ($k$), as well as the recovery rate ($\alpha_1$) and the mortality rates ($\gamma, \mu$). If $R_0 < 1$ the transmission dies out illustrating the stability of DFE ($E_0$) and the disease persists when $R_0 > 1$ indicating that the transmission converges to the model's EE ($E_1$).

### 4.2 Codimension 1 Bifurcation Analysis

We conducted a bifurcation analysis in XPPAUT using parametrisation as in Table 1. The aim is to explore how variations in the epidemiological parameters influence the system's behaviour. In codimension 1 bifurcation analysis, Figure 2 is obtained where the vertical axis represents the infected population ($I$). The horizontal axis represents the intervention levels ($k$), which often include measures like vaccination policy, quarantine efforts, or social distancing intensity in an epidemiological system.

Table 1: Table of Parameter Values [1]

| Parameter | Value | Dimension |
|---|---|---|
| A | 1.75 | Individuals/Time |
| $\beta$ | 0.01 | (individualsxtime)$^{-1}$ |
| k | 2 | Individual $^{-1}$ |
| $\mu$ | 0.005 | Time$^{-1}$ |
| $\alpha_0$ | 0.2 | Time$^{-1}$ |
| $\alpha_1$ | 0.21 | Time$^{-1}$ |
| b | 0.2 | Individuals |
| $\gamma$ | 0.2 | Time $^{-1}$ |

The system exhibits a threshold at $k_{BP}$, i.e., the critical value of the parameter $k$, which corresponds to a transcritical (or forward) bifurcation. There are two key types of equilibria: (i) disease-free equilibrium (DFE) and (ii) endemic equilibrium (EE). Generally, the red (respectively, black) line indicates stable (respectively, unstable) DFE. With high (respectively, low)

intervention levels, $k > k_{BP}$ (respectively, $k < k_{BP}$), the spread of disease can (respectively, cannot) be controlled in a long run. Similar observations hold for EE, where red (respectively, black) line indicates stable (respectively, unstable) equilibrium.

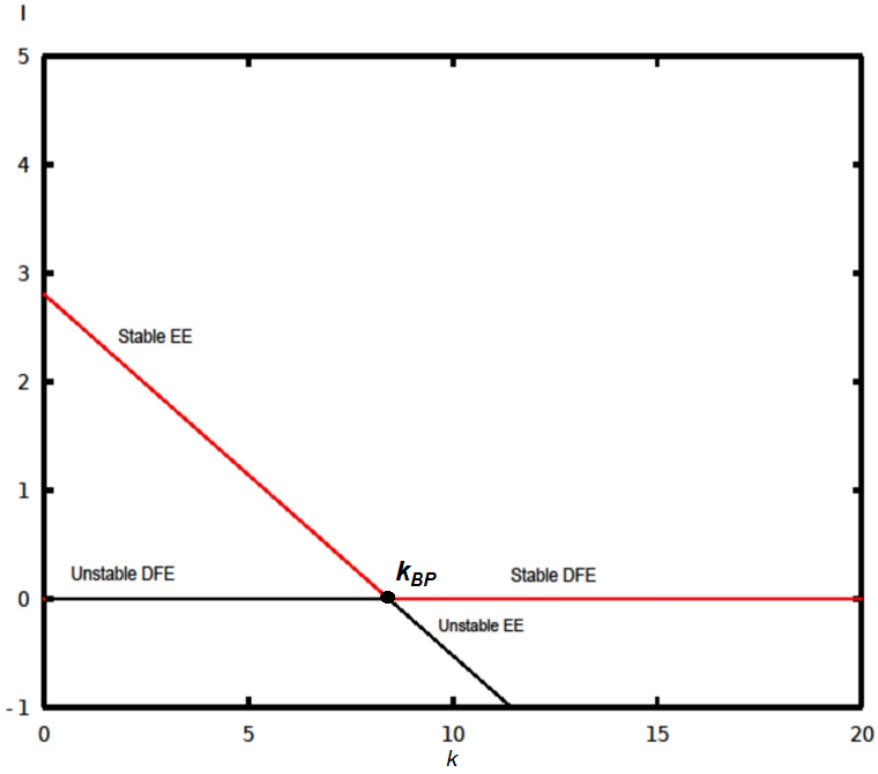


Figure 2: Codimension 1 using $k$ as the bifurcation parameter.

At the threshold point $k_{BP}$, the system undergoes an exchange of stability between equilibria. When the intervention level crosses this threshold from left to right, the stability of the disease-free equilibrium shifts from unstable to stable. This indicates that as control measures surpass a certain effectiveness threshold i.e., $k > k_{BP}$, the system will move towards disease elimination. Below this threshold i.e., $k < k_{BP}$, the system remains in an endemic state where the disease persists in the population (stable EE). This means that without sufficient intervention, the infection continues to circulate within the population.

To better understand the effect of distinct factors in determining the dynamics of the system, in the next codimension 1 bifurcation analysis, represented by Figure 3, we examine how the changes in recovery rate, $\alpha_1$, can lead to different epidemiological outcomes of the system. This bifurcation diagram is divided into several regions, each representing a different qualitative behaviour of the system. The $x$-axis represents the recovery rate $\alpha_1$, while the $y$-axis shows the infected population, $I$. Several bifurcation points such as transcritical ($\alpha_{1\ BP}$), Hopf bifurcation ($\alpha_{1\ HB}$) and saddle-node ($\alpha_{1\ LP}$) bifurcations, and different equilibrium states (both stable and unstable) are observed.

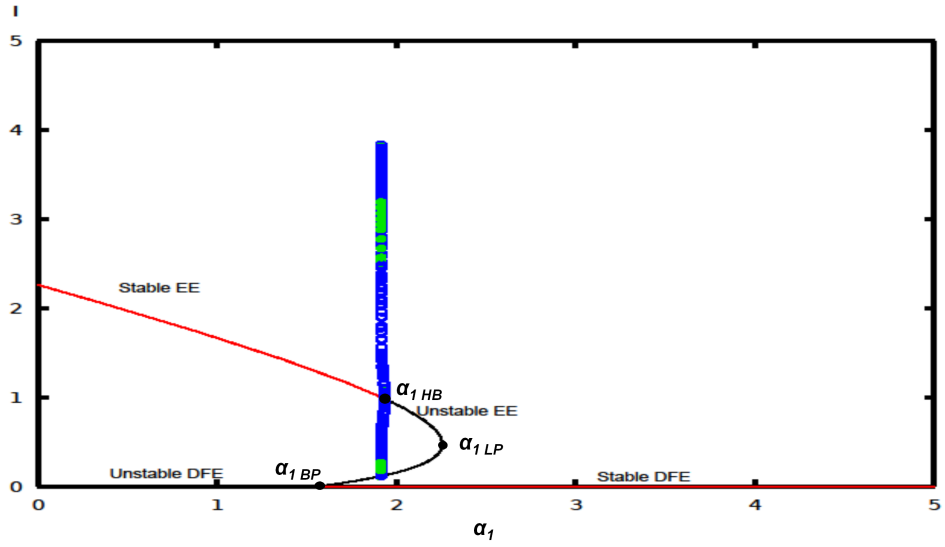


Figure 3: Codimension 1 using $\alpha_1$ as the bifurcation parameter.

*Region* $\alpha_1 < \alpha_{1\ BP}$*:* For small values of recovery force, i.e., to the left of transcritical bifurcation ($\alpha_{1\ BP}$), the system exhibits a stable endemic equilibrium (EE), where the infected population maintains a positive density. This observation is indicated by the red curve in this region. As $\alpha_1$ increases, the infected population slowly decreases, suggesting that a higher recovery rate leads to a reduction in the endemic level of the infection.

*Region* $\alpha_{1\ BP} < \alpha_1 < \alpha_{1\ HB}$*:* As shown by Figure 3, the system exhibits alternative stable states between disease-free and endemic equilibria, along with oscillatory solutions, depending on initial conditions. The oscillation is induced by a Hopf bifurcation ($\alpha_{1\ HB}$) where this bifurcation gives rise to oscillations in the infected population, as indicated by Figure 4 with stable (green) and unstable (blue) oscillatory dynamics. At the collision point of stable and unstable oscillations, a saddle-node bifurcation of limit cycles (LPC) arises. These oscillatory solutions (represented by Figure 5) correspond to the aforementioned limit cycles, which suggest periodic outbreaks of the infection as $\alpha_1$ varies within this realistic range. The presence of both stable and unstable equilibria together with limit cycles indicates complex dynamical behaviour in this epidemiological system.

*Region* $\alpha_1 > \alpha_{1\ HB}$*:* As $\alpha_1$ further increases beyond Hopf bifurcation (HB) point, the system transitions toward a stable disease-free equilibrium (DFE). The population oscillations disappear, and the infected population converges to zero, marking the eradication of the disease in the population. This is indicated by the flat line at $I = 0$. For high values of $\alpha_1$, the system remains in a stable disease-free state (DFE). In this situation, the recovery rate is sufficiently high that the infection cannot persist in the population.

This co-dimension 1 bifurcation analysis reveals that the dynamical behaviours of the system are highly sensitive to changes in the recovery rate $\alpha_1$. For low values of $\alpha_1$, the infection persists in the population (endemic equilibrium). As $\alpha_1$ increases, the system undergoes several bifurcations, leading alternative stable states between DFE, EE and oscillatory behavior. At higher recovery rates, the eradication of the disease is possible. Understanding these is crucial for designing effective intervention strategies to control the spread of the infection.

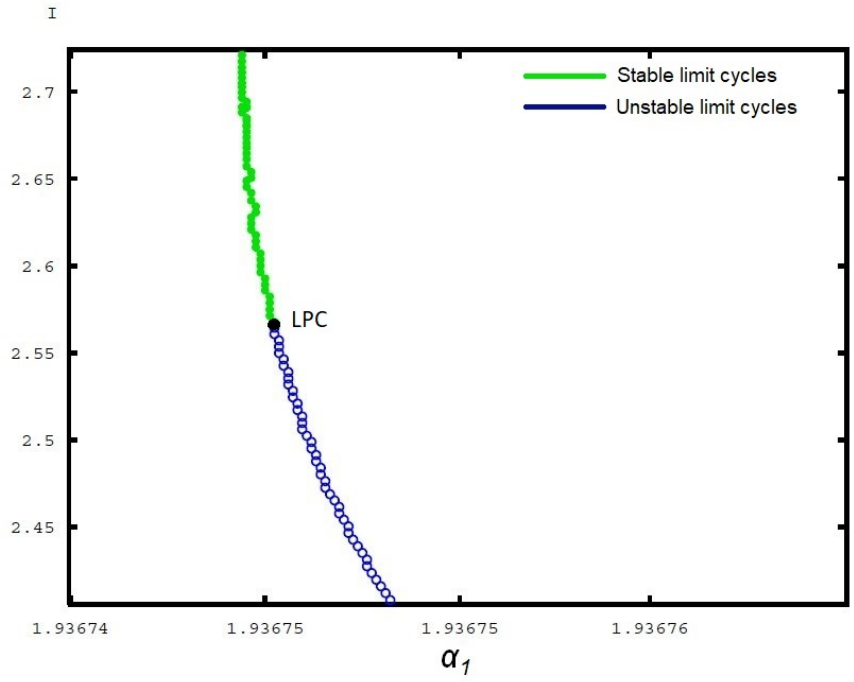


Figure 4: Existence of both stable and unstable limit cycles.

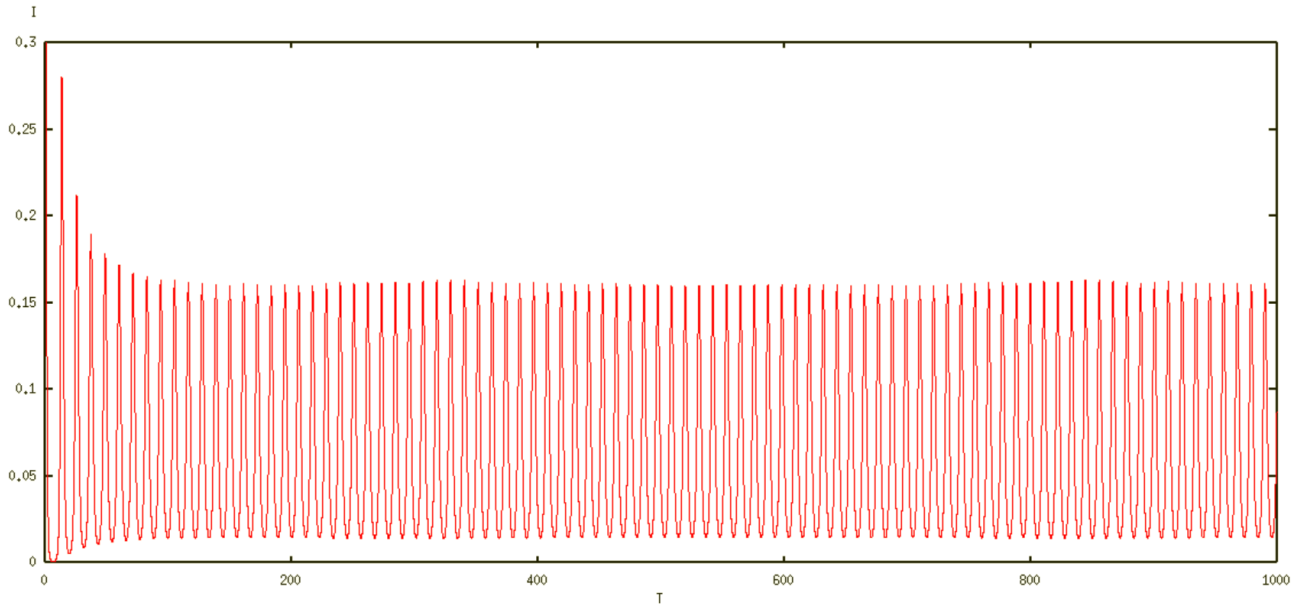


Figure 5: Oscillatory dynamics in this epidemiological system.

### 4.3 Codimension 2 Bifurcation Analysis

To better understand the combined influences between distinct intervention levels $k$ and recovery forces $\alpha_1$, we performed codimension 2 bifurcation analysis by varying these two epidemiological parameters simultaneously. Figure 6 illustrates the possible dynamical behaviours using different colored curves to represent various types of bifurcations.

The blue curve indicates Hopf bifurcation (HB), where the system transitions from a stable state to oscillatory behavior, potentially leading to periodic outbreaks. The red curve represents saddle-node bifurcation, where two endemic equilibria collide and annihilate each other. Then, the cyan curve denotes transcritical bifurcation, where the stability of EE and DFE equilibrium points is swapped.

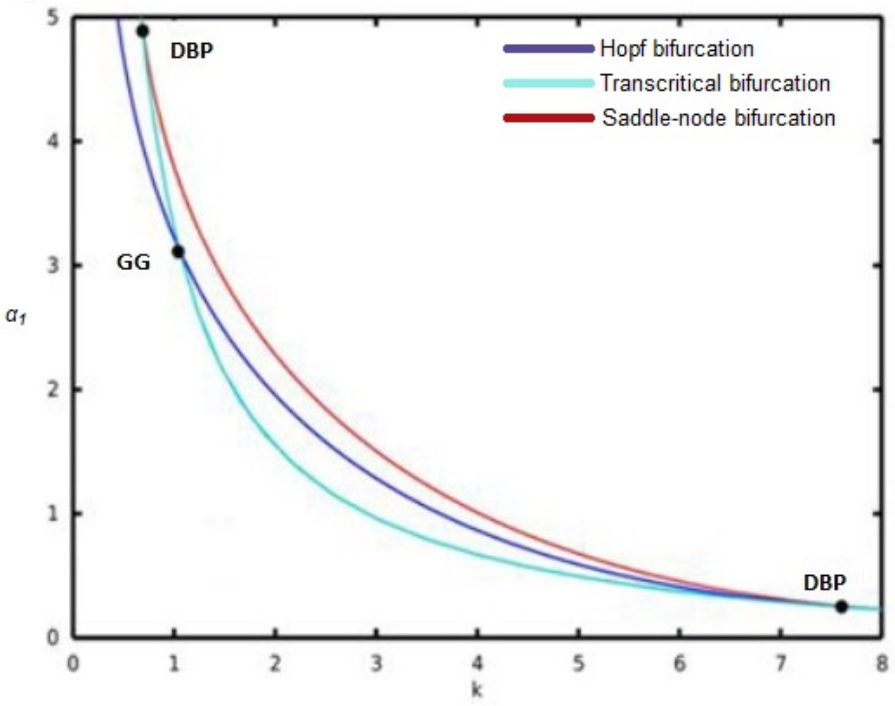


Figure 6: Codimension 2 bifurcation analysis combining both $k$ and $\alpha_1$ as bifurcation parameters.

The figure also highlights the emergence of codimension two bifurcation points corresponding to degenerate transcritical bifurcations ($DBP$) at the intersection of the saddle-node and transcritical bifurcation curves. This type of bifurcation indicates that small changes in the transmission and recovery rates can lead to significant alterations in the system's behavior, potentially causing sudden shifts in disease dynamics.

Additionally, there emerges another codimension two point corresponding to a Gavrilov Guckenheimer bifurcation (GG): at this point, the Hopf bifurcations intersect the transcritical bifurcation. This complex bifurcation scenario demonstrates that the system can exhibit both stable and unstable limit cycles together with the existence of alternative stable states between distinct equilibria, leading to the (dis-)appearance of endemic equilibria and periodic outbreaks.

Overall, the codimension two bifurcations that emerge in this system act as organising centers and separate the parameter space into several regions with different epidemiological outcomes. The analysis also reveals that even slight variations in important epidemiological parameters like recovery rates can have profound impacts on the stability and behavior of the system, highlighting the need for adaptive and dynamic intervention strategies in public health policy.

## 5 Conclusion

This study demonstrates a numerical bifurcation analysis of an $SIR$ model incorporating a Monod-type nonlinear incidence rate and a nonlinear recovery rate. The analysis reveals critical insights into the system's dynamics and stability.

The bifurcation analysis is essential for identifying the epidemiological tipping (or bifurcation) points during outbreaks. The appearance of stable and unstable equilibria due to transcritical bifurcation, along with the emergence of limit cycles from Hopf bifurcation points, demonstrate the complexity of disease dynamics. Additionally, the presence of degenerate transcritical and Gavrilov-Guckenheimer bifurcations illustrates the potential for sudden and dramatic changes in disease dynamics, emphasising the need for adaptive and dynamic intervention strategies.

Overall, this analysis offers valuable insights for public health policy, particularly in understanding how variations in intervention levels and recovery rates can influence the stability and prevalence of infectious diseases. This work also highlights the importance of mathematical modeling and dynamical systems techniques in investigating the interplay among various epidemiological factors, thereby offering valuable insights to guide effective epidemic control strategies.

**Acknowledgments**

The authors acknowledge support from the Fundamental Research Grant Scheme with Project Code: FRGS/1/2022/STG06 /USM/02/1 by the Ministry of Higher Education, Malaysia (MOHE).

## References

[1] Alshammari, F. S. and Khan, M. A. Dynamic Behaviors of a Modified SIR-Based COVID-19 Model with Nonlinear Incidence and Recovery Rates. *Alexandria Engineering Journal*. 2021. 60: 2997–3005.

[2] Shan, C. and Zhu, H. Bifurcations and complex dynamics of an SIR model with the impact of the number of hospital beds. *Journal of Differential Equations*. 2014. 257: 1662–1688.

[3] Khan, I. U., Qasim, M., El Koufi, A., and Ullah, H. The Stability Analysis and Transmission Dynamics of the SIR Model with Nonlinear Recovery and Incidence Rates. *Mathematical Problems in Engineering*. 2022. 60.

[4] Li, G.-H. and Zhang, Y.-X. Dynamic behaviors of a modified SIR model in epidemic diseases using nonlinear incidence and recovery rates. *PLOS ONE*. 2017. 12: 1–28.

[5] Li, S. SIR Epidemic Model with General Nonlinear Incidence Rate and Lévy Jumps. *Mathematics*. 2024. 12: 1–21.

[6] Ahmed, M., Bin Masud, M. A., and Sarker, M. M. A. Bifurcation Analysis and Optimal Control of Discrete SIR Model for COVID-19. *Chaos, Solitons and Fractals*. 2023. 174: 1–10.

[7] Idisi, O. I., Yusuf, T. T., Owolabi, K. M., and Ojokoh, B. A. A bifurcation analysis and model of COVID-19 transmission dynamics with post-vaccination infection impact. *Healthcare Analytics*. 2023. 3: 1–15.

[8] Ajbar, A., Alqahtani, R., and Boumaza, M. Dynamics of a Modified SIR-Based COVID-19 Model with Linear Incidence Rate and Nonlinear Removal Rate, and Public Awareness. *Frontiers in Physics*. 2021. 9: 1–12.

[9] Yu, X., Liu, M., Zheng, Z., and Hu, D. Complex dynamics of a discrete-time SIR model with nonlinear incidence and recovery rates. *International Journal of Biomathematics*. 2023. 16.

[10] Ullah, I., Ali, N., Haq, I. U., Ahmad, I., Albalwi, M. D., and Biswas, M. H. A. Analysis of COVID-19 Disease Model: Backward Bifurcation and Impact of Pharmaceutical and Nonpharmaceutical Interventions. *International Journal of Mathematics and Mathematical Sciences*. 2024. Article ID 6069996.

[11] Devi, A. and Gupta, P. K. Bifurcation Analysis of a COVID-19 Dynamical Model in the Presence of Holling Type-II Saturated Treatment with Reinfection. *Iranian Journal of Science*. 2024. 9: 161–179.

[12] Kotola, B. S., Teklu, S. W., and Abebaw, Y. F. Bifurcation and optimal control analysis of HIV/AIDS and COVID-19 co-infection model with numerical simulation. *PLOS ONE*. 2023. 18: 1–47.

[13] Chhetri, B. and Dasu, K. K. V. Stability and bifurcation analysis of a nested multi-scale model for COVID-19 viral infection. *Computational and Mathematical Biophysics*. 2024. 12: 1–29.

[14] Maurício de Carvalho, J. P. S. and Rodrigues, A. A. SIR Model with Vaccination: Bifurcation Analysis. *Qualitative Theory of Dynamical Systems*. 2023. 22: 105.

[15] Cui, Q., Qiu, Z., Liu, W., and Hu, Z. Complex Dynamics of an SIR Epidemic Model with Nonlinear Saturate Incidence and Recovery Rates. *Entropy*. 2017.

[16] Dubey, B., Dubey, P., and Dubey, U. S. Dynamics of an SIR Model with Nonlinear Incidence and Treatment Rate. *Applications and Applied Mathematics: An International Journal (AAM)*. 2015. 10.

[17] Momani, S., Batiha, I. M., Hijazi, M. S., Bendib, I., Ouannas, A., and Anakira, N. Fractional-Order SEIR Model for COVID-19: Finite-Time Stability Analysis and Numerical Validation. *International Journal of Neutrosophic Science (IJNS)*. 2025. 26.

[18] Xu, S. and Hu, Y. Dynamic analysis of a Caputo fractional-order SEIR model with a general incidence rate. *Mathematics*. 2025. 15: 1–19.